Journal of Hazardous Materials Letters 4 (2023) 100084

Contents lists available at ScienceDirect

Journal of Hazardous Materials Letters

journal homepage: www.sciencedirect.com/journal/journal-of-hazardous-materials-letters

The influence of chain length on the sorption of C4-C10 perfluorocarboxylic acids during transport in a sand

Ying Lyu [a,b,c,*], Baohua Wang [a,b,d], Mark L. Brusseau [e,**]

[a] Key Lab of Groundwater Resources and Environment, Ministry of Education, Jilin University, Changchun 130026, PR China
[b] Jilin Provincial Key Laboratory of Water Resources and Environment, Jilin University, Changchun 130026, PR China
[c] Institute of Water Resources and Environment, Jilin University, Changchun 130026, China
[d] Shen Zhen LiYuan Water Design & Consultation CO., LTD, China
[e] Environmental Science Department, University of Arizona, 429 Shantz Bldg, USA

ARTICLE INFO

Keywords:
PFCAs
PFAS
PFOA
Retention

ABSTRACT

The impact of chain length on the retention and transport of perfluorocarboxylic acids (PFCAs) in a quartz sand was investigated. Short-chain (C4–C7: PFBA, PFPeA, PFHxA, PFHpA) and long-chain (C8–C10: PFOA, PFNA, PFDA) PFCAs were selected as a representative homologous series. Miscible-displacement transport experiments were conducted under saturated conditions to characterize the magnitudes of sorption mediating retention and transport. Quantitative-structure/property-relationship (QSPR) analysis was applied to characterize the influence of molecular size on sorption. The transport of the long-chain PFCAs exhibited greater retardation than the short-chain PFCAs. The log of the equilibrium sorption coefficient (K_d) exhibited a biphasic relationship with carbon number and molar volume, with the magnitude of measured sorption for the short-chain PFCAs significantly greater than would be predicted using the QSPR regression developed for the long-chain PFCAs. This is consistent with batch-measured data reported in the literature, and likely reflects the relative influence of different sorption mechanisms for the short-chain vs long-chain PFCAs.

1. Introduction

Per- and poly-fluoroalkyl substances (PFAS) are contaminants of critical concern that are documented to be widespread in the environment. Numerous field studies have demonstrated the presence of PFAS in soils across the globe, as reported in a recent meta-analysis (Brusseau et al., 2020). Therefore, the transport of PFAS in soil and groundwater is one current focus of research. PFAS are amphiphilic molecules containing fluoroalkyl groups of different chain lengths and structures. The transport and fate behavior of PFAS is known to be a function in part of chain length. For example. the impact of chain length on the sorption of PFAS by soils and sediments has been investigated in several studies, with the results generally showing increased sorption for longer-chain PFAS (e.g., Higgins and Luthy, 2006; Guelfo and Higgins, 2013; McLachlan et al., 2019; Nguyen et al., 2020). Notably, some studies have reported that the sorption of short-chain PFAS deviates from the behavior measured for long-chain PFAS (e.g., Guelfo and Higgins, 2013; McLachlan et al., 2019; Nguyen et al., 2020). These observations have significant implications for the prediction of sorption coefficients using the standard approach that is based on the assumption that soil organic carbon controls sorption. However, it is critical to point out that all of these studies have been conducted using batch sorption measurements. Conversely, there has been minimal investigation of the impact of chain length on PFAS sorption under dynamic transport conditions.

Vierke et al. (2014) investigated the transport of several PFAS in a sand-packed column representing a riverbank filtration scenario. Retardation factors and K_d values were reported, but correlations between K_d and chain length were not presented. The transport of several PFAS in a loamy sand was investigated with a focus on chemical oxidant impacts (McKenzie et al., 2015). Retardation factors were reported, but there was no assessment of correlations between K_d and chain length. Guelfo et al. (2020) examined the transport of several PFAS in four porous media. Retardation factors were not determined from the transport data, and therefore no correlations between K_d and chain length were presented. Qi et al. (2022) examined the transport of two short-chain and two long-chain PFAS in an acid-treated sand. The two

* Corresponding author at: Key Lab of Groundwater Resources and Environment, Ministry of Education, Jilin University, Changchun 130026, China.
** Corresponding author.
E-mail addresses: yinglyu@jlu.edu.cn (Y. Lyu), brusseau@arizona.edu (M.L. Brusseau).

https://doi.org/10.1016/j.hazl.2023.100084
Received 4 May 2023; Received in revised form 25 July 2023; Accepted 18 August 2023
Available online 19 August 2023

short-chain PFAS and the smaller long-chain PFAS exhibited minimal sorption as a result of the acid treatment, with the authors noting the breakthrough curves for those three were similar to that of the nonreactive tracer. No testing was done of potential correlations between K_d and chain length. The preceding demonstrates that no studies to date have employed transport-measured sorption data to specifically examine correlations between K_d and chain-length properties for PFAS.

The objective of this research is to examine the impact of chain length on sorption of PFAS during transport in a well-characterized sand. Short-chain (C4–C7: PFBA, PFPeA, PFHxA, PFHpA) and long-chain (C8–C10: PFOA, PFNA, PFDA) PFCAs are selected as a representative homologous series of PFAS. Miscible-displacement transport experiments are conducted to characterize the magnitude of sorption. Quantitative-structure/property-relationship (QSPR) analysis is applied to characterize the influence of molecular size (chain length) on sorption. PFCA transport is simulated using a mathematical model that accounts for nonlinear, rate-limited sorption. The results are compared to another set of transport data reported in the literature.

2. Materials and methods

The C4–C10 homologous series of perfluorocarboxylic acids (PFCAs) was selected as representative short-chain and long-chain PFAS. The standardized nomenclature for chain length is employed, with $n < 7$ fluorinated carbons defined as short-chain PFCAs (Buck et al., 2011). Perfluorobutanoic acid (PFBA, $C_4HF_7O_2$, CAS#375-22-4; 98 % purity), perfluoropentanoic acid (PFPeA, $C_5HF_9O_2$, CAS# 2706-90-3; 97 % purity), perfluorohexanoic acid (PFHxA, $C_6HF_{11}O_2$, CAS# 307-24-4; 97 % purity), perfluoroheptanoic acid (PFHpA, $C_7HF_{13}O_2$, CAS#375-85-9; 99 % purity), and perfluorooctanoic acid (PFOA, $C_8HF_{15}O_2$, CAS#335-67-1; 96 % purity) were purchased from sigma-Aldrich; perfluorononanoic acid (PFNA, $C_9HF_{17}O_2$, CAS#375-95-1; 97 % purity) was purchased from Shanghai Macklin Biochemical Co., Ltd; perfluorodecanoic acid (PFDA, $C_{10}HF_{19}O_2$, CAS#335-76-2; 98 % purity) was purchased from Shanghai Aladdin Biochemical Technology Co., Ltd. Pentafluorobenzoic acid, a non-PFAS compound that is commonly used as a nonreactive tracer was used in this study. A background electrolyte solution was developed using sodium chloride (ionic strength = 0.01 M, pH = 7) to be consistent with prior PFAS studies. All of the solutions were prepared using boiled ultra-pure water to eliminate the influence of air in the solutions. A commercially available natural quartz sand with a median grain diameter of 0.35 mm was used for the experiments. This medium has been used in our prior studies (Lyu et al., 2018).

The columns were 15 cm long with inner diameter of 1.6 cm, and constructed of acrylic. Flow distributors were placed on the top and at the bottom of the column to promote uniform fluid distribution and to support the media. Peristaltic pumps (BT100-02, Baoding Qili Precision Pump Co., Ltd., China) were used to provide fluid flow. All experiments were conducted at room temperature (20 ± 1 °C).

The experiments were conducted using methods we have used in previous studies (Lyu et al., 2018; Brusseau et al., 2019; Wang et al., 2021). The miscible-displacement experiments were conducted with each respective PFCA present alone in solution, rather than employing a multiple-component PFCA solution. This was done to eliminate potential co-solute interactions, allowing direct focus on chain-length impacts on transport. A concentration of 1 mg/L was used for each PFCA to be consistent with our prior study (Lyu et al., 2018). This value is consistent with soil porewater concentrations that are anticipated to be comparatively high in source zones at sites for which aqueous film-forming foams (AFFF) have been used. Porewater concentrations may range into the mg/L range based on reported soil concentrations that range up to the 10′s to 100′s of mg/kg (Brusseau et al., 2020). Such high concentrations have been demonstrated in a recent study, wherein measured porewater concentrations ranging up to > 10 mg/L were reported for an AFFF-impacted source zone (Anderson et al., 2022). Furthermore, groundwater concentrations ranging into several mg/L have been reported for aquifers in the vicinity of AFFF sources (Johnson et al., 2022).

The sand was packed uniformly into the column, after which the electrolyte solution was introduced at a low flow rate from the bottom of the vertically oriented column. Once the column was saturated, the solution containing a given PFAS was injected into the bottom of the column. The volume of solution injected was sufficient to allow the effluent concentration of the PFAS to attain the injection concentration. After this point, solution with no PFAS was injected to displace the PFAS solution. Effluent samples were collected periodically for subsequent analysis. Breakthrough curves were developed by plotting relative concentration (quotient of effluent and injection concentrations) vs nondimensional time (pore volumes). The volume of solution discharged from the column was divided by the retention volume of the column (resident pore volume) to determine the eluted pore volumes.

The PFAS were analyzed by high-performance liquid chromatography (Thermo Model U3000, USA) and tandem mass spectrometry (TSQ quantum, Thermo Scientific, USA), i.e., LC-MS/MS. An Agilent C18 column (Hypersil GOLD VANQUIS, 1.9 μm, 100 × 2.1 mm) was used, with the column temperature set and maintained at 50 °C. The dual mobile phase comprised 5 mM ammonium acetate and acetonitrile applied in a 60:40 gradient at a flow rate of 0.3 mL/min. Each column effluent sample was filtered by membrane and then injected directly, with injection volumes of 1 μL. Test results revealed the absence of any interferences associated with the membrane. The quantitative detection limit (QDL) for the method is approximately 1 μg/L. Background aqueous samples collected from the column effluent before injection of PFAS revealed no measurable PFAS concentrations or other interferences for all experiments.

Measured retardation factors were determined for each miscible-displacement experiment by the standard methods of calculating the area above the breakthrough curve (frontal analysis) and temporal moment analysis. These methods have been demonstrated to be robust for PFAS applications (Brusseau et al., 2019; Van Glubt et al., 2021). A one-dimensional numerical model that couples steady-state flow and advective and dispersive transport is used to simulate the PFCA transport (Brusseau, 2020). Details of the model are presented in the cited source. The model accounts for nonlinear, rate-limited sorption. This model has been demonstrated to provide accurate simulations of PFAS and hydrocarbon-surfactant transport measured in miscible-displacement experiments (Brusseau, 2020; Brusseau et al., 2021). The QSPR analysis was conducted using methods employed in our prior works (Brusseau, 2019a,b).

3. Results and discussion

The breakthrough curves (BTCs) for transport of the nonreactive tracer are sharp and symmetrical, with retardation factors of 1 (data not shown). The BTCs for the PFCAs exhibit moderate amounts of asymmetry and concentration tailing (see Fig. 1 for illustration). The effluent recoveries averaged 99.5 % (± 3 % 95 % confidence interval). This indicates the absence of measurable mass loss via transformation, irreversible sorption, or experimental artifacts. The magnitudes of retention and associated retardation factors increased with chain length (Table 1). Retardation was low to moderate overall, with retardation factors ranging from 1.2 to 1.3 for the C4–C7 and ranging from 1.4 to 2.6 for C8–C10.

The simulations produced with the mathematical model incorporating a two-domain representation of nonlinear, rate-limited sorption provide good matches to the measured BTCs. Root mean square errors range from 0.033 to 0.064 (Table 1), corresponding to a mean %-RMSE of approximately 9 %. One set of simulations was conducted with sorption treated as nonlinear and another set with sorption treated as linear. The two sets of simulations are essentially identical, indicating that nonlinear sorption contributed minimally to the asymmetry and tailing of the BTCs. This is consistent with the shapes of the

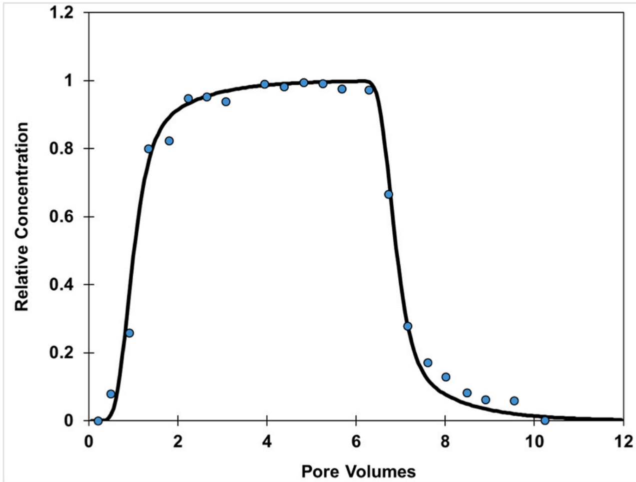

Fig. 1. Measured and simulated breakthrough curves for transport of C4 to illustrate asymmetry and tailing.

Table 1
Retardation factors and K_d values.

PFCA	Measured R[a]	K_d (cm^3/g)	Predicted K_d[a] (cm^3/g)	% Error[b]	RMSE[c]
C4	1.23	0.068	0.005	92.2	0.035
C5	1.25	0.073	0.01	86.4	0.049
C6	1.28	0.078	0.02	75.8	0.033
C7	1.30	0.084	0.04	53.0	0.042
C8	1.38	0.099	0.09	11.0	0.050
C9	1.56	0.157	0.18	14.1	0.064
C10	2.60	0.426	0.38	10.9	0.049

[a] Kd value predicted using the molar volume regression established for the long-chain PFAS in Fig. 3B.
[b] Percent error between predicted and measured K_d.
[c] Root mean square error for transport model simulation of measured breakthrough curve.

breakthrough curves, wherein concentration tailing is observed for both the arrival and elution fronts. The impact of nonlinear sorption produces a self-sharpening arrival front and an extended-tail elution front when the Freundlich N coefficient is less than one. Conversely, the observation of tailing for both the arrival and elution fronts is consistent with the impact of sorption kinetics. As noted, the mass recoveries were close to 100 %, indicating no measurable impact of irreversible sorption. Based on all of these results, the observed nonideal transport is attributed to rate-limited sorption. This is consistent with prior modeling of PFAS transport data in sands and soils (Brusseau et al., 2019; Brusseau, 2020; Guelfo et al., 2020; Wang et al., 2021).

The K_d values determined from the transport experiments are presented in Table 1. The value measured for PFOA, 0.099 cm^3/g, is essentially identical to the K_d determined from batch and column isotherms measured for PFOA sorption by the sand reported in our prior study (Van Glubt et al., 2021). Specifically, an effective K_d of 0.098 was determined for an input concentration of 1 mg/L. The concurrency of PFOA K_d values obtain in this study to our prior batch and column isotherm data indicates excellent consistency of the methods.

The log K_d values as a function of carbon number and molar volume are presented in Fig. 2. A biphasic relationship is observed, with the short-chain PFCAs exhibiting an approximately 10-times smaller slope than the long chains. Transport-measured data for sorption of PFOS by the same sand is also presented in Fig. 2. The log K_d for PFOS is consistent with the correlation determined for the long-chain PFCAs, indicating that the same functional relationship governs both the PFCAs and PFOS irrespective of their different headgroups.

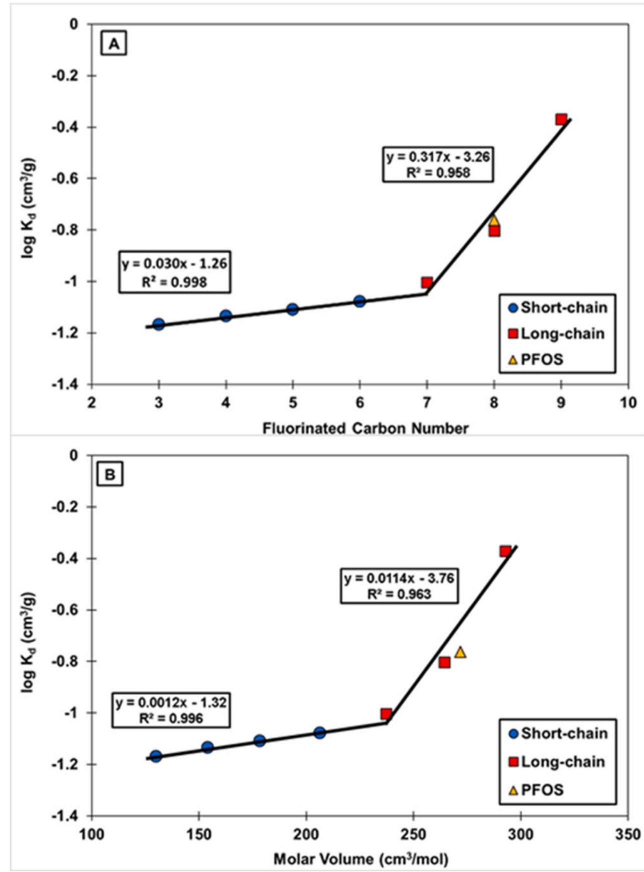

Fig. 2. log K_d of PFCAs as a function of (A) carbon number (for the chain) and (B) molar volume. PFOS data from Van Glubt et al. (2021).

The results presented in Fig. 2 are consistent with the results of prior batch-mode studies wherein the sorption of short-chain PFAS did not follow the same trend as that of the long-chains (Guelfo and Higgins, 2013; Nguyen et al., 2020). The correlation of K_d values to chain-length properties such as molecular weight, fluorinated carbon number, and molar volume are hypothesized to indicate that sorption is mediated by the hydrophobic-interaction mechanism (Higgins and Luthy, 2006; Guelfo and Higgins, 2013; Brusseau, 2019b). The differential sorption behavior of short-chain PFAS is attributed to the contributions of additional sorption mechanisms, such as electrostatic interactions with inorganic components of the soil (Guelfo and Higgins, 2013).

The influence of the observed differential sorption behavior is illustrated by comparing K_d values measured for the short-chain PFAS to predicted K_d values estimated with the molar-volume-based QSPR regression determined for the long-chain PFCAs (Fig. 2B). The K_ds predicted for the short-chain PFCAs range from factors of ∼ 2 to ∼ 10 smaller than the measured values, and %-errors range from 53 % to 92 % (Table 1). Conversely, the predicted values are reasonably close to the measured values for the longer-chain PFCAs, with %-errors of 11–14 %. This indicates that empirical relationships developed for long-chain PFAS may not always be representative for those with shorter chains.

As noted in the Introduction, McKenzie et al. (2015) conducted a set of miscible-displacement experiments to investigate the transport of several PFAS in a loamy sand. They reported retardation factors but did not evaluate correlations between K_d and chain length. We have calculated K_d and corresponding K_{oc} values from their reported retardation factors and plot the latter as a function of molar volume (Fig. 3). The log K_{oc} values for their long-chain PFAS are observed to be a uniform function of molar volume. Conversely, the value for the one short-chain

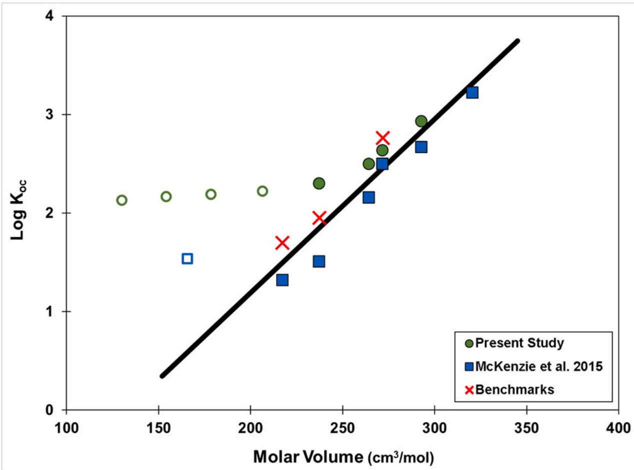

Fig. 3. Plot of organic-carbon normalized sorption coefficients (K_{oc}) versus molar volume. The long-chain and short-chain PFAS are the filled and open symbols, respectively. The benchmark values represent measurements of PFAS (PFHxS, PFOA, PFOS) sorption by humin (Zhao et al., 2014) and peat (Zhi and Liu, 2018); values determined for 50 μg/L, the approximate geomean of the injection concentrations for the two transport studies.

PFAS available (SD>mean) appears to deviate from the long-chain function.

The log K_{oc} values for all but the smallest long-chain PFAS are similar for the two sets of data. This demonstrates consistency in measured sorption behavior obtained for the two transport studies. Notably, the McKenzie et al. study employed injection concentrations of ~ 2 μg/L for their transport experiments. The consistency between the two sets of data indicates that the aqueous concentration difference between the two studies is not important for measured sorption behavior in these particular systems. This is congruent with the results of the transport modeling that revealed minimal impact of nonlinear sorption.

Also plotted in Fig. 3 are three benchmark log K_{oc} values determined from experiments measuring PFAS sorption by organic media (humin and peat). The log K_{oc} values for the long-chain PFAS from the two transport studies are relatively consistent with the benchmark values, which suggests that sorption is controlled by organic carbon via hydrophobic interaction for the two media. Soil organic carbon has been demonstrated in prior studies to control the hydrophobic-interaction mediated sorption of long-chain anionic PFAS (e.g., Higgins and Luthy, 2006; Milinovic et al., 2015; Nguyen et al., 2020; Oliver et al., 2020). The deviation of the short-chain PFAS from the benchmarked long-chain QSPR function supports the hypothesis that additional sorption mechanisms are influencing their sorption.

4. Conclusions

The transport of a homologous series of PFCAs ranging from C4 to C10 was investigated. The long-chain PFCAs exhibited greater retardation than the short-chain PFCAs. The BTCs exhibited a moderate degree of asymmetry, indicating transport was influenced to some extent by rate-limited sorption. The log of the equilibrium sorption coefficient (K_d) exhibited a biphasic relationship with carbon number and molar volume, with the magnitude of measured sorption for the short-chain PFCAs significantly greater than would be predicted using the QSPR regression developed for the long-chain PFCAs. Data from a prior PFAS transport study was shown to exhibit similar results. These observations, which are the first reported based on transport-generated measurements, are consistent with batch-measured data reported in the literature. The behavior likely reflects the relative influence of different sorption mechanisms for the short-chain vs long-chain anionic PFAS. These results suggest that the sorption of shorter-chain PFAS may be greater in some cases than anticipated, and that estimates based on empirical or anecdotal observations of longer-chain PFAS may not be representative in those circumstances.

Funding Information

This work was supported by the Natural Science Foundation of Jilin Provincial Science & Technology Department (#20230101084JC), the Thirteenth Five-Year Science and Technology Project of Jilin Province Education Department (#JJKH20201005KJ), National Natural Science Foundation of China (#41902247), and the Hydrologic Sciences Program of the NSF (2023351).

Declaration of Competing Interest

The authors declare that they have no known competing financial interests or personal relationships that could have appeared to influence the work reported in this paper.

Data Availability

All data are presented in the manuscript.

Acknowledgements

This work was supported by the Natural Science Foundation of Jilin Provincial Science & Technology Department (#20230101084JC), the Thirteenth Five-Year Science and Technology Project of Jilin Province Education Department (#JJKH20201005KJ), National Natural Science Foundation of China (#41902247), and the Hydrologic Sciences Program of the NSF (2023351). We thank the reviewers for their constructive comments.

References

Anderson, R.H., Feild, J.B., Dieffenbach-Carle, H., Elsharnouby, O., Krebs, R.K., 2022. Assessment of PFAS in collocated soil and porewater samples at an AFFF-impacted source zone: field-scale validation of suction lysimeters. Chemosphere 308, 136247.
Brusseau, M.L., 2019a. The influence of molecular structure on the adsorption of PFAS to fluid-fluid interfaces: using QSPR to predict interfacial adsorption coefficients. Water Res. 152, 148–158.
Brusseau, M.L., 2019b. Estimating the relative magnitudes of adsorption to solid-water and air/oil-water interfaces for per- and poly-fluoroalkyl substances. Environ. Pollut. 254, 113102.
Brusseau, M.L., 2020. Simulating PFAS transport influenced by rate-limited multi-process retention. Water Res. 168, 115179.
Brusseau, M.L., Khan, N., Wang, Y.K., Yan, N., Van Glubt, S., Carroll, K.C., 2019. Nonideal transport and extended elution tailing of PFOS in soil. Environ. Sci. Technol. 53, 10654–10664.
Brusseau, M.L., Anderson, R.H., Guo, B., 2020. PFAS concentrations in soils: background levels versus contaminated sites. Sci. Total Environ. 740, 140017.
Brusseau, M.L., Guo, B., Huang, D., Yan, N., Lyu, Y., 2021. Ideal versus nonideal transport of PFAS in unsaturated porous media. Water Res. 202, 117405.
Buck, R.C., Franklin, J., Berger, U., Conder, J.M., Cousins, I.T., de Voogt, P., Jensen, A.A., Kannan, K., Mabury, S.A., van Leeuwen, S.P., 2011. Perfluoroalkyl and polyfluoroalkyl substances in the environment: terminology, classification, and origins. Integr. Environ. Assess. Manag. 7 (4), 513–541. https://doi.org/10.1002/ieam.258.
Guelfo, J.L., Higgins, C.P., 2013. Subsurface transport potential of perfluoroalkyl acids at aqueous film-forming foam (AFFF)-impacted sites. Environ. Sci. Technol. 47 (9), 4164–4171.
Guelfo, J.L., Wunsch, A., Mccray, J., Stults, J.F., Higgins, C.P., 2020. Subsurface transport potential of perfluoroalkyl acids (PFAAs): column experiments and modeling. J. Contam. Hydrol. 233, 9–20.
Higgins, C.P., Luthy, R.G., 2006. Sorption of perfluorinated surfactants on sediments. Environ. Sci. Technol. 40, 7251–7256.
Johnson, G.R., Brusseau, M.L., Carroll, K.C., Tick, G.R., Duncan, C.M., 2022. Global distributions, source-type dependencies, and concentration ranges of per- and polyfluoroalkyl substances in groundwater. Sci. Total Environ. 841, 156602.
Lyu, Y., Brusseau, M.L., Chen, W., Yan, N., Fu, X., Lin, X., 2018. Adsorption of PFOA at the air-water interface during transport in unsaturated porous media. Environ. Sci. Technol. 52, 7745–7753.
McKenzie, E.R., Siegrist, R.L., McCray, J.E., Higgins, C.P., 2015. Effects of chemical oxidants on perfluoroalkyl acid transport in one-dimensional porous media columns. Environ. Sci. Technol. 49, 1681–1689.

McLachlan, M.S., Felizeter, S., Klein, M., Kotthoff, M., de Voogt, P., 2019. Fate of perfluoroalkyl acid mixture in an agricultural soil studied in lysimeters. Chemosphere 223, 180–187.

Milinovic, J., Lacorte, S., Vidal, M., Rigol, A., 2015. Sorption behaviour of perfluoroalkyl substances in soils. Sci. Total Environ. 511, 63–71.

Nguyen, T.M.H., Braunig, J., Thompson, K., Thompson, J., Kabiri, S., Navarro, D.A., Kookana, R.S., Grimison, C., Barnes, C.M., Higgins, C.P., McLaughlin, M.J., Mueller, J.F., 2020. Influences of chemical properties, soil properties, and solution pH on soil-water partitioning coefficients of per- and polyfluoroalkyl substances (PFASs). Environ. Sci. Technol. 54 (24), 15883–15892.

Oliver, D.P., Navarro, D.A., Baldock, J., Simpson, S.L., Kookana, R.S., 2020. Sorption behaviour of per- and polyfluoroalkyl substances (PFASs) as affected by the properties of coastal estuarine sediments. Sci. Total Environ. 720.

Qi, L., Li, R., Wu, Y., Lin, X., Chen, G., 2022. Effect of solution chemistry on the transport of short-chain and long-chain perfluoroalkyl carboxylic acids (PFCAs) in saturated porous media. Chemosphere 303, 135160.

Van Glubt, S., Brusseau, M.L., Yan, N., Huang, D.D., Khan, N., Carroll, K.C., 2021. Column versus batch methods for measuring PFOS and PFOA sorption to geomedia. Environ. Pollut. 268, 115917.

Vierke, L., Moller, A., Klitzke, S., 2014. Transport of perfluoroalkyl acids in a water-saturated sediment column investigated under near-natural conditions. Environ. Pollut. 186, 7–13.

Wang, Y., Khan, N., Huang, D., Carroll, K.C., Brusseau, M.L., 2021. Transport of PFOS in aquifer sediment: transport behavior and a distributed-sorption model. Sci. Total Environ. 779, 146444.

Zhao, L., Zhang, Y., Fang, S., Zhu, L., Liu, Z., 2014. Comparative sorption and desorption behaviors of PFHxS and PFOS on sequentially extracted humic substances. J. Environ. Sci. 26, 2517–2525.

Zhi, Y., Liu, J., 2018. Sorption and desorption of anionic, cationic and zwitterionic polyfluoroalkyl substances by soil organic matter and pyrogenic carbonaceous materials. Chem. Eng. J. 346, 682–691.